



## Genome biology of the Darkedged Splitfin, *Girardinichthys multiradiatus*, and the evolution of sex chromosomes and placentation

Kang Du, Martin Pippel, Susanne Kneitz, et al.

*Genome Res.* published online January 26, 2022

Access the most recent version at doi:[10.1101/gr.275826.121](https://doi.org/10.1101/gr.275826.121)

---

<b>P&lt;P</b>	Published online January 26, 2022 in advance of the print journal.
<b>Accepted Manuscript</b>	Peer-reviewed and accepted for publication but not copyedited or typeset; accepted manuscript is likely to differ from the final, published version.
<b>Creative Commons License</b>	This article is distributed exclusively by Cold Spring Harbor Laboratory Press for the first six months after the full-issue publication date (see <a href="https://genome.cshlp.org/site/misc/terms.xhtml">https://genome.cshlp.org/site/misc/terms.xhtml</a> ). After six months, it is available under a Creative Commons License (Attribution-NonCommercial 4.0 International), as described at <a href="http://creativecommons.org/licenses/by-nc/4.0/">http://creativecommons.org/licenses/by-nc/4.0/</a> .
<b>Email Alerting Service</b>	Receive free email alerts when new articles cite this article - sign up in the box at the top right corner of the article or <a href="#">click here</a> .

---



---

To subscribe to *Genome Research* go to:  
<https://genome.cshlp.org/subscriptions>

---

Published by Cold Spring Harbor Laboratory Press

1                   **Genome biology of the Darkedged Splitfin,**  
2                   ***Girardinichthys multiradiatus*, and the evolution of sex**  
3                   **chromosomes and placentation**

4  
5 Kang Du<sup>1</sup>, Martin Pippel<sup>2</sup>, Susanne Kneitz<sup>3</sup>, Romain Feron<sup>4</sup>, Irene da Cruz<sup>5</sup>, Sylke  
6 Winkler<sup>2</sup>, Brigitta Wilde<sup>3</sup>, Edgar G. Avila Luna<sup>6</sup>, Gene Myers<sup>2\*</sup>, Yann Guiguen<sup>7\*</sup>,  
7 Constantino Macias Garcia<sup>6\*</sup>, Manfred Schartl<sup>1,5,#</sup>

8 <sup>1</sup>The Xiphophorus Genetic Stock Center, Department of Chemistry and Biochemistry,  
9 Texas State University, San Marcos, Texas, TX 78666, USA

10 <sup>2</sup>Max-Planck Institute of Molecular Cell Biology and Genetics, Pfotenhauerstraße 108,  
11 10307 Dresden, Germany

12 <sup>3</sup>Biochemistry and Cell Biology, Biocenter, University of Wuerzburg, Am Hubland,  
13 97074 Wuerzburg, Germany

14 <sup>4</sup>Department of Ecology and Evolution, University of Lausanne, and Swiss Institute of  
15 Bioinformatics, 1015 Lausanne, Switzerland

16 <sup>5</sup>Developmental Biochemistry, Biocenter, University of Wuerzburg, Am Hubland, 97074  
17 Wuerzburg, Germany

18 <sup>6</sup>Instituto de Ecología, Universidad Nacional Autónoma de México, Ciudad Universitaria,  
19 Circuito exterior s/n anexo al Jardín Botánico C. P. 04510, Mexico City D. F, Mexico

20 <sup>7</sup>INRAE, LPGP, Rennes, France

21 \*Equally contributing senior authors

22 #Corresponding author

23

## 24 **Abstract**

25 Viviparity evolved independently about 150 times in vertebrates and over 20 times in  
26 fish. Several lineages added to the protection of the embryo inside the body of the mother  
27 the provisioning of nutrients and physiological exchange. This often led to the evolution  
28 of a placenta. Amongst fish, one of the most complex systems serving the function of the  
29 placenta is the embryonal trophotaenia/ovarian luminal epithelium of the Goodeid fishes.  
30 For a better understanding of this feature and others of this group of fishes, high quality  
31 genomic resources are essential. We have sequenced the genome of the darkedged  
32 splitfin, *Girardinichthys multiradiatus*. The assembly is chromosome-level and includes  
33 the X and Y Chromosomes. A large male-specific region on the Y was identified  
34 covering 80% of Chromosome 20, allowing some first inferences on the recent origin and  
35 a candidate male sex determining gene. Genome-wide transcriptomics uncovered sex  
36 specific differences in brain gene expression with an enrichment for neurosteroidogenesis  
37 and testis genes in males. The expression signatures of the splitfin embryonal and  
38 maternal placenta showed overlap with homologous tissues including human placenta,  
39 the ovarian follicle epithelium of matrotrophic Poeciliid fish species and the brood pouch  
40 epithelium of the seahorse. Our comparative analyses on the evolution of embryonal and  
41 maternal placenta indicate that the evolutionary novelty of maternal provisioning  
42 development repeatedly made use of genes which already had the same function in other  
43 tissues. In this way already pre-existing modules are assembled and repurposed to  
44 provide the molecular changes for this novel trait.

45 **Keywords: Goodeids, placenta, trophotaenia, sex chromosome, transcriptome,**  
46 **brain, whole genome sequencing, chromosome assembly.**

## 47 **Introduction**

48 Viviparity, a mode of reproduction that can exacerbate the conflict between sexes over  
49 the allocation of resources to offspring, has evolved independently amongst all classes of  
50 jawed vertebrates (except birds) about 150 times, 21 of which occurred in fish (for review  
51 see (Blackburn 2015)). Viviparous species can be arranged along a continuum from  
52 lecithotrophic to matrotrophic based on whether the nutrients required for embryonic  
53 development are present in the egg (lecithotrophic development), or whether they are

54 gradually provided by the mother through gestation (matrotrophic development), for  
55 instance via a placenta (placentotrophy) (Blackburn 1999; Ghalambor et al. 2004; Pollux  
56 et al. 2009). In spite of the large number of independent origins, our understanding of the  
57 evolutionary and functional development of matrotrophic viviparity, especially of that  
58 involving a placenta, comes mostly from the study of mammalian matrotrophy, and while  
59 vast, our knowledge of its genomic underpinning is limited to only one transition from  
60 oviparity to matrotrophic viviparity and a few recent studies on fish (see below) (Lynch  
61 et al. 2008; Kin et al. 2016). There is hence a need to incorporate more taxa to the study  
62 of the evolution of viviparity, ideally taxa which include both oviparous and viviparous  
63 (matrotrophic) species. Fish in the Order Cyprinodontiformes seem appropriate to  
64 conduct such comparisons, as different forms of viviparity have evolved independently in  
65 several families: Poeciliidae, Jenynsiidae, Anablepidae and Goodeidae (Meyer and  
66 Lydeard 1993) (Blackburn 2015). Accordingly, comparative analyses revealed that  
67 placentation drives a shift from a reliance on pre-zygotic mate choice to increasing levels  
68 of polyandry, in conjunction with post-zygotic mechanisms of mate selection (Pollux et  
69 al. 2014; Furness and Capellini 2019). More recently, comparative transcriptomic  
70 analyses have found parallels between poecilid and mammalian placental viviparity  
71 (Guernsey et al. 2020). By focusing on the speciose Poeciliidae, this study explored the  
72 consequences of several transitions between lecithotrophy and matrotrophy, although still  
73 only covering one transition between oviparity and viviparity. It is likely due to the lack  
74 of genomic resources that the family Goodeidae has not been used to investigate the  
75 genomic background of the transition from oviparity to placental viviparity. The  
76 Goodeidae is a small, yet diverse family of Cyprinodontiformes native to North America  
77 (Parenti 1981). The subfamily Empetrichthynae, from Nevada in the USA, includes two  
78 genera of oviparous fish, and the subfamily Goodeinae from Central Mexico includes  
79 ~40 viviparous species distributed in 16 genera (Webb et al. 2004). This high ratio of  
80 genera to species is indicative of a burst of diversification (Mayr 1942), which has been  
81 identified as an adaptive radiation following the evolution of viviparity (Ritchie et al.  
82 2005). There are at present no genomic resources that may allow the use of the  
83 Goodeidae to explore the genomic transitions that accompanied the evolution of  
84 matrotrophic viviparity from oviparity.

85 Matrotrophy in goodeids is linked to the possession of a dynamic placenta sensu  
86 Mossmann (Mossman 1991) made up of a maternal part, the internal ovarian epithelium,  
87 and an embryonic component, the trophotaenia (Lombardi and Wourms 1985; Uribe MC  
88 2005; Schindler 2015) (Fig. 1). The latter are extensions of the embryonic hindgut mostly  
89 shaped in the form of ribbons or rosettes (Turner 1937; Lombardi and Wourms 1985)  
90 made of an absorptive epithelium around a well vascularized core (Mendoza 1972;  
91 Lombardi and Wourms 1985). The maternal part of the placenta is represented by the  
92 follicular epithelium of the ovary, which is closely associated with the trophotaenia. This  
93 is a dynamic system because early embryos rely on an initial supply of yolk, then develop  
94 the trophotaenia that reaches out to the modified ovarian lumen epithelium, but starts to  
95 regress, possibly through apoptosis, as gestation draws to an end (Iida et al. 2015).  
96 Maternally provided proteins, which can include vitellogenin (Vega-López et al. 2007)  
97 and also residues of dead siblings (Greven and Grossherr 1992), are uptaken by the  
98 trophotaenial epithelium via receptor-mediated endocytosis, and subjected to lysosomal  
99 degradation (Schindler and De Vries 1987; Schindler and Kujat 1990; Schindler 2003).

100 Unlike other viviparous fish such as poeciliids (Constantz 1984), splitfin females do not  
101 store sperm (BISAZZA 1997), and they are only receptive for about one week after  
102 giving birth, which takes place every two months (Macías-García and Saborío 2004).  
103 Additionally, males lack an intromittent organ, thus sperm is deposited in the outer part  
104 of the gonopore (BISAZZA 1997; Garcia and Valero 2010; Greven and Brenner 2010).  
105 These particularities of splitfin reproductive biology may promote that males adjust their  
106 sperm production and mating effort to the probability of finding mates and of facing  
107 sperm competition (Simmons and Fitzpatrick 2012), enforcing novel conditions for  
108 sperm to reach the ova. Thus in addition to the consequences for females, it is likely that  
109 viviparity has also left a genomic footprint on males.

110 Splitfin males are heavily ornamented (Ritchie et al. 2005; Méndez-Janovitz et al. 2019)  
111 and, as they cannot force copulations (see previous paragraph) they perform complex  
112 courtship displays to secure mating (Macías-García and Saborío 2004). This  
113 preponderance of sexual selection may be related to high rates of differentiation, as  
114 previously proposed (Darwin 1896; Panhuis et al. 2001; Ritchie 2007).

115 Mexican goodeids face a variety of environmental challenges (De La Vega-Salazar et al.  
116 2003; DOMÍNGUEZ-DOMÍNGUEZ et al. 2006), including chemical pollution (Marina  
117 et al. 1997), which has made splitfins a model for ecotoxicological research (Arellano-  
118 Aguilar and Macías Garcia 2008; Arellano-Aguilar and Macias Garcia 2008; Rueda-Jasso  
119 et al. 2014; Guerrero-Estévez and López-López 2016).

120 Here we report the first high-quality reference genome of a Goodeid, the darkedged  
121 splitfin (also known as Amarillo), *Girardinichthys multiradiatus*, assembled at full  
122 chromosome level including the X and Y Chromosomes. Using this genomic resource,  
123 we uncovered a pronounced sex difference in brain transcriptomes and established the  
124 expression signature of the trophotaenial placenta showing considerable overlap with  
125 human placenta and RNA-seq data from another livebearing fish and seahorse.

## 126 **Results**

### 127 **Genome sequencing, chromosome assembly and annotation**

128 To obtain a genome assembly of high contiguity and completeness, we used the pipelines  
129 of the international Vertebrate Genome Project that incorporate state-of-the-art  
130 sequencing technologies and assembly algorithms (Rhie et al. 2021). Pacific Biosciences  
131 (PacBio) continuous long reads (71-fold coverage), 10x Genomics Illumina read clouds  
132 (52 fold coverage), Bionano optical maps (1870 fold coverage) and chromosome  
133 conformation capture (Hi-C) Illumina read pairs (94 fold coverage) from three male  
134 individuals were generated (Supplemental Tables S1, S2). The PacBio reads were  
135 assembled into contigs using the customized assembler Damar  
136 (<https://github.com/MartinPippel/Damar>). Next, we used the 10x Illumina read-cloud  
137 data to correct base errors and phase haplotypes, arbitrarily picking one haplotype in a  
138 phased block. Finally, we used Bionano optical maps and then Hi-C data to produce long-  
139 range scaffolds. This resulted in a final assembly of 1.1 Gb with a contig N50 of 17 Mb,  
140 arranged in 71 scaffolds. Of these, 24 are chromosome-size (Fig. 2) in agreement with the  
141 karyotype of *G. multiradiatus* (Uyeno et al. 1983), making up 99.7% of the genome  
142 assembly (Supplemental Table S3).

143 A comparison with other teleost chromosome assemblies disclosed a high degree of  
144 conserved synteny not only to other Cyprinodontiformes (*Fundulus*, *Xiphophorus* and  
145 medaka), but also with the more distant Perciformes and to a lower extent with mostly  
146 small translocations and rearrangements to herring, cavefish and zebrafish (Fig. 3). To  
147 annotate protein coding genes, gene evidence from protein homology of other species,  
148 RNA-seq transcriptomes from darkedged splitfin and ab-initio predictions were  
149 integrated. A total of 23770 protein coding genes were annotated. The BUSCO  
150 completeness based on the actinopterygii\_odb9 dataset was improved from 96.4% to  
151 99.3% by the annotation process (Supplemental Table S4). Out of the 23770 genes,  
152 23463 (98.7%) have a BLAST hit to the Swiss-Prot/RefSeq database. 2113 (8.9%) of the  
153 protein-coding genes are single exon genes. Additionally, 1900 tRNA, 21 rRNA, 279  
154 miRNA and 355 other non-coding RNA genes were annotated (Supplemental Table S5)

## 155 **Genome evolution**

156 The genome of *G. multiradiatus* consists of 37.3% of repetitive sequences according to  
157 RepeatMasker (Supplemental Table S6). This is in the range of many other teleost fish  
158 genomes (Shao et al. 2018) including in the closely related *Fundulus* and Medaka species  
159 but considerably higher than the livebearing platyfish. Of note, there is a strong  
160 expansion of ERV class I elements, which is not found in other genomes of the order  
161 Cyprinodontiformes (2.5% vs 0.01- 0.4%). The transposon landscape history  
162 (Supplemental Fig. S1) indicates that darkedged splitfin experienced a strong wave of TE  
163 expansion rather recently, in contrast to other teleosts genomes analyzed so far.

164 A phylogenomics reconstruction of the evolutionary relationships of splitfin to other  
165 teleosts using a gene set of 1425 high quality orthologs confirmed previous groupings.  
166 The tree revealed a split of the Goodeid branch from egg-laying cyprinodonts around 52  
167 MYA, about twice the age estimated from partial mitochondrial sequences (Webb et al.  
168 2004). The last common ancestor of Goodeids with the livebearing Poeciliids dated back  
169 almost to the same period, around 64 MYA (Fig. 3, Supplemental Fig. S2).

170 Gene family analysis revealed that 42 gene families expanded and 128 contracted in the  
171 splitfin genome. However, none of these families shows a dynamic exclusive to the  
172 lineage of *G. multiradiatus* (Supplemental Fig. S2).

### 173 **Sex-biased gene expression in brain**

174 The availability of an annotated genome allowed us to look for sexual dimorphism of the  
175 brain on a molecular level. Differential gene expression analyses of female and male  
176 brain transcriptomes revealed that 324 genes, with a  $\log_2$  fold change (FC)  $>1$  and  
177 adjusted p-values  $<0.05$ , were more expressed in males, while only 42 genes showed a  
178 biased expression towards females (Supplemental Table S7). In the female brain *foxl2a*,  
179 which is a main transcription factor in female gonad development, was higher expressed  
180 than in males. Enrichment for Gene Ontology terms revealed functions related to  
181 membrane structure and function including transporter activities (Supplemental Fig. S3A-  
182 D). The male biased genes were enriched for several categories related to germ cell  
183 development, male meiosis and spermatogenesis (Supplemental Fig. S3E-G). Amongst  
184 these are *dmrt1*, an important regulator of male sexual development in fish, and genes  
185 that function in the early stage of meiosis, e.g. *spo11*, *sycp1*, *sycp2*, *sycp3*, *hormad1*, or  
186 sperm development, e.g. *spata4*, *spata7*, *spata17*, *spata22*, *spefl*, *spag6*, *spag8*. Of note,  
187 also genes from the piRNA pathway (*exd1*, *piwill*, *tdrd5*, *tdrd6*, *tdrd9*), which is  
188 particularly active in testes, are predominantly expressed in male brain. Several genes of  
189 steroidogenesis pathways were also upregulated in male (*dhrs11b*, *akr1a1b*, *cyp11c1*).

### 190 **Placental development**

191 The placenta is an organ formed by the sustained apposition or fusion of fetal membranes  
192 and parental tissue for physiological exchange (Mossman 1991). Goodeids have been  
193 described as having the most complex placental organ amongst livebearing fishes to  
194 support the developing embryos, given its large array of histological and cytological  
195 modifications of the intra-ovarian epithelium and the trophotaenial absorptive  
196 epithelium, which are apposed to each other during pregnancy (Uribe et al. 2010;  
197 Schindler 2015). To contribute to the understanding of the evolution, function and  
198 development of this outstanding trait, we analyzed transcriptomes of the trophotaenia

199 (embryonal part of placenta) and the ovary after dissecting out the embryos (maternal  
200 part of the placenta). Both datasets were then compared to all other transcriptomes (male  
201 and female brains, testis, organ mix, early and late embryos and trophotaeniae or ovary,  
202 respectively). Trophotaenia and ovary predominant expression signatures were defined  
203 by a  $\log_2$  fold change  $>2$  compared to all other transcriptomes in accordance with the  
204 definition of “genes preferentially expressed in human placenta”  
205 (<https://www.proteinatlas.org/humanproteome/tissue/placenta>). This revealed 1653  
206 trophotaenia and 1132 ovary enhanced genes (Supplemental Tables S8, S9).

207 The ovarian transcriptome is enriched for genes with functions for formation of the zona  
208 pellucida and extracellular matrix, fertilization, immune response and steroidogenesis  
209 (Supplemental Fig. S4). The most upregulated gene in the ovary is *cyp19a1a*  
210 ( $\log_2FC=7.46$ ), the ovarian isoform of the estrogen producing enzyme aromatase.

211 The genes that constitute the expression signature of the trophotaenia are highly enriched  
212 for genes with a function in brush border membranes, transport of ions and metabolites,  
213 and metabolic pathways (Supplemental Fig. S4) in agreement with the role of the  
214 embryonal part of a placenta. Of note, the telomerase reverse transcriptase is highly  
215 upregulated ( $\log_2FC=5.82$  compared to all other organs), as well as the gene encoding the  
216 prolactin receptor ( $\log_2FC=4.41$ ).

217 Insulin-like growth factor 2 (IGF2) signaling has an important role in regulating placental  
218 supply of nutrients in mammals and is a key gene undergoing paternal imprinting  
219 (DeChiara et al. 1990; DeChiara et al. 1991). In the darkedged splitfin the *insulin-like*  
220 *growth factor-binding protein1-like* and *insulin-like growth factor-binding protein4-like*  
221 genes are predominantly expressed in the trophotaenia and *insulin-like growth factor-*  
222 *binding protein 1* and *3*, *insulin-like growth factor 1*, and *IGF-like family receptor 1* are  
223 predominantly expressed in the ovary. However, *igf2* is not expressed in the ovary and  
224 also not part of the trophotaenia transcriptome.

225 We then checked the trophotaenia and ovary transcriptomes for expression of other genes  
226 imprinted in mammals (N=255, <https://www.geneimprint.com/site/genes-by-status>) and

227 found that 16 of these are expressed in trophotaenia and 10 in ovary (Supplemental Table  
228 S10)

229 In another family of livebearing cyprinodontiform fishes, the Poeciliidae, several species  
230 have evolved maternal provisioning of nutrients to the developing embryo throughout  
231 pregnancy. Here, the follicular epithelium like in splitfins is the maternal part of the  
232 placenta supplying support. We compared the transcriptomes of follicles of the  
233 matrotrophic species *Poeciliopsis retropinna* (Guernsey et al. 2020) with our dataset.  
234 1640 genes were found to be overexpressed in follicles of *P. retropinna* compared to  
235 follicles of the lecithotrophic species *P. turrubarensis*, and among those 59 overlapped  
236 with the ovary-specific expression pattern of *G. multiradiatus* (Supplemental Fig. S5;  
237 Supplemental Table S11). The shared genes are enriched for extracellular matrix and  
238 cytokine signalling related GO terms (Supplemental Fig. S6A).

239 The lineage of seahorses has also developed livebearing, convergently. In addition,  
240 seahorses have evolved provisioning of nutrients to the embryo by a specialization of the  
241 ventral skin integument, the male brood pouch epithelium, representing the parental part  
242 of the placenta (Griffith and Wagner 2017). A transcriptomic study identified 147  
243 significantly upregulated genes in the pregnant (compared with the nonpregnant) and  
244 post-parturition seahorse brood pouch (compared with the late-pregnant). (Whittington et  
245 al. 2015). Nine of these are also upregulated in the ovary of splitfin (Supplemental Fig.  
246 S7) with functions in calcium and lipid transport and tissue remodeling.

247 The human placenta is formed from the endometrium as the maternal part and the  
248 trophoblast, which develops into the embryonal contribution of the placenta. The  
249 available human placenta transcriptome combines the embryonal and maternal part. Thus,  
250 we compared it to both parts of the splitfin placenta. The trophotaenia and ovary  
251 transcriptomes of the splitfin overlap with 89 of the 493 genes of the human placenta  
252 transcriptome(<https://www.proteinatlas.org/>) (Supplemental Fig. S8A; Supplemental  
253 Table S12). These include the vascular endothelial growth factor family member  
254 placental growth factor (PGF), the prolactin receptor and many components of the  
255 extracellular matrix and genes enriched for GO terms angiogenesis, growth and  
256 morphogenesis (Supplemental Fig. S6B,C). A comparison of trophotaenia with the

257 human trophoblast, which gives rise to the embryonal part of the placenta, revealed 97  
258 genes in common between both tissues (Supplemental Table S12, Supplemental Fig.  
259 S8B) including many transporters and transcription factors enriched again for  
260 morphogenesis, extracellular matrix and angiogenesis GO terms (Supplemental Fig.  
261 S6D).

262 The evolution of a highly sophisticated placental organ mediating matrotrophy in  
263 Goodeids may have required changes in protein structure and function that should be  
264 visible as signatures of positive selection. To uncover such genomic traces of natural  
265 selection we collected 7102 one-to-one orthologs from *G. multiradiatus* and 11 other  
266 teleost species (Supplemental Fig. S2) including the livebearing species from the  
267 Poeciliidae family and the more distantly related seahorse and tested these genes for  
268 positive selection in *G. multiradiatus*. With site class 2a (positive selection in marked  
269 branch and conserved in rest) we identified 48 genes and with site class 2b (positive  
270 selection in marked branch and relaxed in rest) 122 genes under positive selection  
271 specifically in the splitfin lineage (Supplemental Table S13). These genes include 16  
272 from the trophotaenia and 6 from the ovary-specific transcriptomes (Supplemental Table  
273 S14).

274 The positive selection analysis revealed 440 genes (site class 2a, 128 genes, 2b, 312  
275 genes) in seahorse (Supplemental Table S15). In *Poeciliopsis* because of the  
276 unavailability of an annotated genome the orthologous genes could only be identified by  
277 a BLAST to the genome assembly. This restricted the number of one-to-one orthologs for  
278 comparison with splitfin to about one quarter (n=1521) of which 65 genes (site class 2a,  
279 35 genes, 2b, 30 genes) are under positive selection (Supplemental Table S16). Between  
280 all three species, there are two genes commonly under positive selection in *Poeciliopsis*  
281 and splitfin, 8 genes shared between seahorse and splitfin and one gene, *sterol-O-*  
282 *acyltransferase 1*, which is under positive selection in all three species (Supplemental  
283 Fig. S9).

284 **Sex determination and sex chromosomes**

285 To characterize the sex determination system of the darkedged splitfin we first searched  
286 for sex-linked markers using Restriction site Associated DNA Sequencing (RAD-seq)  
287 (Feron et al. 2021) in 29 females and 27 males. A total of 6,359,801 markers was found,  
288 of which 892 were significantly associated with male phenotype ( $p < 0.05$ , chi-square test  
289 with Bonferroni correction) and none were associated with female phenotype (Fig. 4A;  
290 Supplemental Table S17). These results suggested a stable male heterogametic genetic  
291 sex determination system. The absence of outliers most likely indicates the absence of  
292 relevant environmental factors or autosomal modifiers influencing the XY sex  
293 chromosomal system.

294 We then aligned these RAD-seq markers to the genome assembly of darkedged splitfin.  
295 Among the 892 markers significantly associated with male phenotype, 675 (76%) were  
296 aligned to a unique position with mapping quality higher than 20, and of these good  
297 quality markers 654 (97%) were aligned to scaffold 20 in a region ranging from 22 kb to  
298 34.5 Mb (Fig. 4B-C). These results indicate that scaffold 20 is the sex chromosome in  
299 darkedged splitfin and that a large region spanning 80% of the sex chromosome is  
300 differentiated between the X and Y Chromosomes.

301 To identify the male specific region and to elucidate the evolution of the sex  
302 chromosomes of splitfin, a haplotype-resolved assembly of scaffold 20 was done.  
303 Mapping of the male-specific RAD-tags identified the putative Y Chromosome (Fig. 5A),  
304 where 645 (71%) had a significant hit.

305 Sequence difference between X and Y was determined in 10 kb sliding windows as the  
306 percentage of SNP and indels. It uncovered a large region from 0 - 34.5 Mb on the Y,  
307 where the nucleotide difference was uniformly in the range of 1.4% (Fig. 5B). Beyond  
308 this point the overall sequence difference between X and Y was close to zero. The  $d_S$   
309 values were high in the XY-differential region (Median 0.01) and low in the terminal  
310 segment (Supplemental Fig. S10A). The  $d_N/d_S$  values in the terminal region are  
311 predominantly around 0.2 indicating purifying selection. Most genes in the XY-  
312 differential region have on average twice as high values and many close to 1 or even  
313 higher, indicating relaxation from purifying selection (Supplemental Fig. S10B).  
314 Together this identifies a possible terminal pseudoautosomal region of 7 Mb with about

315 200 genes and a large region on the Y of about 34.5 Mb containing around 900 genes,  
316 where it is different from the X (Supplemental Fig. S10C).

317 To estimate the age of the Y we used the  $d_S$  distance between the X and Y in the  
318 differential region and calibrated it to the  $d_S$  based divergence time estimate of splitfin to  
319 *Fundulus* (52.6 Mya, see Supplemental Fig. S2). This revealed that the Y Chromosome  
320 of splitfin originated only about 2 Mya (Supplemental Fig. S11).

321 The region on the Y which is different from the X does not have a higher content of  
322 repeats and TE's. Also, the transposon landscape is similar to the corresponding region  
323 on the X and all autosomes except for a slightly higher percentage of LINE elements  
324 (Supplemental Fig. S12). The region on the Y has a higher content of pseudogenes  
325 (20.4%) than the corresponding region on the X (13.7%) and all autosomes (16.1%,  
326 Supplemental Methods: Comparison of the X and Y Chromosomes). Mapping the gene  
327 contents of the X and the Y to each other revealed that no gene from the X is missing  
328 from the Y, while there are twelve gene models annotated that are present only on the  
329 male sex chromosome. Manual inspection revealed all of these 12 genes are either  
330 corrupted, pseudogenes or transposon derived sequences (Supplemental Table S18).

331 New sex determining genes arise either from local gene duplications or allelic  
332 diversification (Herpin and Schartl 2008). As we did not find any hint of duplicated Y-  
333 specific genes, we considered that the splitfin male determining gene would show allelic  
334 differentiation between the X and Y copies. We manually checked the 948 genes of the  
335 differentiated region on the Y for the recurrently appearing sex determining genes in  
336 vertebrates. From these (TGF $\beta$  signalling, *dmrt1* and *sox* family members) only *sox8a*,  
337 *sox9a* and *sox10a* are on scaffold 20. While *sox9a* and *sox10a* have  $d_N/d_S$  values of 0.32  
338 and 0.23, which indicate a purifying selection, *sox8a* has a value of 0.81. The X and Y  
339 *sox8a* copies differ by 12 (2.6%) amino acids. Overlaying the computer-modeled protein  
340 structures revealed that none of these differences would compromise the three-  
341 dimensional structure of Sox8a as a whole, suggesting that both copies encode functional  
342 transcription factors (Supplemental Fig. S13). The Y copy presents two amino acid  
343 changes at a highly conserved position (L364M, S360N). The S360N exchange adds a  $\beta$ -  
344 sheet at this place to the secondary structure. Further functional studies are required to

345 elucidate what could be the impact of these changes on Sox8a activity in splitfin. Of note,  
346 the Y allele is preferentially expressed in testis, however, in male brain, the X and Y  
347 alleles are equally expressed (Supplemental Table S19).

## 348 **Discussion**

349 As part of the Vertebrate Genomes Project (VGP), a project of the G10K Consortium,  
350 which aims to generate near error-free reference genome assemblies of ~70,000 extant  
351 vertebrate species, the darkedged splitfin was selected to represent the group of Goodeid  
352 fishes. The availability of a chromosome-level genome assembly of high completeness  
353 allowed us to perform genome-wide analyses to contribute to a better understanding of  
354 several highly interesting characteristics of Goodeids and also benefit ecotoxicological  
355 research.

356 We identified a differentiated XY sex chromosome system in *G. multiradiatus* and  
357 succeeded in assembling X and Y separately. The comparison of these two sex  
358 chromosomes revealed a large MSY with uniform levels of sequence differentiation over  
359 its whole length. Such distribution of male-specific SNPs would be expected if  
360 recombination stopped simultaneously in the Y-specific part by a large chromosomal  
361 inversion. Manual inspection of the Hi-C maps did not support such a single-large  
362 inversion, however, several smaller inversions are possible. Further studies are needed to  
363 explain this pattern.

364 The differentiation of the Y occurred in less than two million years since its origin, about  
365 six MY later than the split between *G. multiradiatus* and its sister species *G. viviparus*  
366 (Webb et al 2004). The two species are different in the expression of epigamic characters,  
367 with *G. multiradiatus* males being more ornamented (larger and colourful median fins)  
368 and having a large repertoire of courtship displays, whereas *G. viviparus* has smaller dark  
369 fins and very simple courtship behaviour (González Zuarth and Macías Garcia 2006;  
370 Méndez-Janovitz and Garcia 2017). A full assembly of the genome of *G. viviparus* is  
371 needed to better understand sex chromosome evolution in the genus *Girardinichthys*.  
372 Comparison of the sex chromosome-specific region to the corresponding region of the *G.*  
373 *multiradiatus* genome can then be used to search for genes involved in male ornaments.

374 Our brain transcriptome analyses uncovered a large number of genes which were more  
375 expressed in males and which are known to fulfill their functions in testis development  
376 and spermatogenesis. This is in agreement with RNA-seq data from human, mouse and  
377 zebrafish (Guo et al. 2003; Guo et al. 2005; Sreenivasan et al. 2008). A closer  
378 relationship of female and male brains to their respective gonad was also reported  
379 (Sreenivasan et al. 2008), however, at least to our knowledge such a strong bias as in  
380 splitfin of male brain towards testis has not been noted. The biological meaning of the  
381 abundance of testis gene expressions in the male brain is unknown as well as its  
382 molecular mechanisms. Shared characteristics between neurons and sperm, including the  
383 importance of the exocytotic process and the presence of similar receptors and signalling  
384 pathways have been hypothesized (Matos et al. 2021). In humans it has been shown that  
385 meiosis genes expressed in the brain are not translated. A possible reason for the absence  
386 of translation of such transcripts to proteins may be connected to the lack of *Dazl*, which  
387 is a key regulator of translation of spermatogenesis genes (Li et al. 2019). In splitfin  
388 brain, *dazl* is expressed only at low levels in male, not at all in females, and abundantly  
389 only in testis. In splitfin, we lack the tools to analyze protein expression, but it may well  
390 be that a large fraction of the testis genes is not translated due to the lack of *Dazl*  
391 (Supplemental Fig. S14). Even if not, all expressed “testis” genes may have a function in  
392 brain they might reflect a co-regulatory expression mechanism, which upregulates genes  
393 that are of importance in both organs, e.g. steroidogenesis genes. The reproductive  
394 biology of splitfins requires a complex male-specific behavior including searching for  
395 receptive females, a whole suite of courtship behaviors (Garcia and Valero 2010) and  
396 constantly adjusting sperm production to suit the current availability of partners and of  
397 potential sperm competitors (Garcia et al. 1998; Simmons and Fitzpatrick 2012) which is  
398 orchestrated in the brain and may be regulated by neurosteroids. We found upregulation  
399 of genes involved in steroidogenesis specifically in the brain of males. Further studies  
400 have to show if these enzymes are indeed involved in the synthesis of neurosteroids.

401 So far, from the other placental fish, seahorse and *Poeciliopsis*, only the parental part of  
402 the placenta was analysed. Here in splitfin, for the first time information also from the  
403 embryonal part could be generated. The placental organ of *G. multiradiatus* shows a high  
404 similarity with the expression signature of human placenta. This is indicative of a

405 convergent evolution of organs that serve embryonic nutrition although they are  
406 phylogenetically quite distant and developmentally totally unrelated. The mammalian  
407 placenta descends from the maternal endometrium and the trophoblast, which have no  
408 counterpart in fish. The goodeid trophotaeniae, however, are outgrowths of the hindgut  
409 that interact with the maternal ovarian wall. The similarities to the human placenta  
410 transcriptome, which is derived from the whole composite organ, are equally shared  
411 between the maternal and embryonal part of the *G. multiradiatus* placenta.

412 The trophotaeniae exhibit a high expression of the prolactin receptor indicating that this  
413 organ is responsive to prolactin stimulation. Prolactin, the lactation hormone of  
414 mammals, is a hormone that plays multiple roles in parental care in fish including: mouth  
415 breeding, nutrient provision by mucus or fluids, parental care behavior and viviparity  
416 (Whittington and Wilson 2013; Dobolyi et al. 2020). Expression of the prolactin receptor  
417 gene has also been observed in the follicular epithelium of matrotrophic *Poeciliopsis*  
418 species (Guernsey et al. 2020). The *prolactin* gene of *G. multiradiatus* is not only  
419 expressed in brain but also at similar levels in trophotaenia and ovary, indicating not only  
420 endocrine but also juxtacrine hormone signaling.

421 The trophotaenia is an embryonic organ and thus high telomerase expression is within  
422 expectation (Wright et al. 1996; Anchelin et al. 2011), in splitfin, its level of expression  
423 achieve 15 – 50 fold higher than in the embryo proper. In the human placenta  
424 dysregulation of telomerase activity is connected to a variety of pregnancy complications  
425 (Fragkiadaki et al. 2016).

426 The absence of *igf2* in the ovary and the trophotaenia of *G. multiradiatus* is intriguing  
427 (Lawton et al. 2005). Parent-of-origin specific expression of this growth factor gene  
428 constitutes an iconic example of imprinting linked to sexual conflict. In mammalian  
429 embryos, the paternal copy can be overexpressed, hence promoting embryo growth  
430 beyond the optimum for the mother, and the maternally inherited copy silenced through  
431 methylation, thus resisting the effects of the paternally-inherited allele. Conversely, the  
432 maternal copy of the cation-independent mannose-6 phosphate receptor, which binds the  
433 growth factor and transports it to lysosomes, is overexpressed, and the paternal allele is  
434 silenced (DeChiara et al. 1990; DeChiara et al. 1991). *Igf2* is expressed in fish embryos

435 (Yuan et al. 2011), including those of *G. multiradiatus*, where there is evidence  
436 suggesting that, as in mammals, the paternal copy is expressed, and the maternal allele is  
437 silenced through methylation (Saldivar Lemus et al. 2017). Thus, we would have  
438 predicted its absence in the ovary transcriptome but expected it to be expressed in the  
439 trophotaenia. At present we have no information of where in the embryo *igf2* is being  
440 expressed, or why it is not being expressed in the trophotaenia, although it is still possible  
441 that its expression in the trophotaenia depends on the developmental stage of the embryo  
442 and that we collected trophotaeniae from embryos of 3-4 and 5-6 weeks of development,  
443 which were, at that stages, not producing this growth factor.

444 Livebearing and maternal or paternal provisioning through placenta-like structures has  
445 evolved independently several times in fish. We asked the question if this physiological  
446 and morphological convergent evolution is connected to similar convergent changes on  
447 the molecular level. Proteins that may have adapted to new functional properties required  
448 for placentation should show signatures of positive selection in the respective lineage.  
449 Indeed, about one fifth of the genes identified as positively selected in splitfin are  
450 specifically expressed in the placenta. An even higher fraction was noted in the  
451 matrotrophic Poeciliid species *Heterandria formosa* (van Kruistum et al. 2019).  
452 However, comparing positively selected genes of seahorse, Poeciliopsis and splitfin  
453 revealed only a single gene in common, *sterol-O-acyltransferase 1*. This gene encodes a  
454 lipid metabolism enzyme, which has a key role as the rate-limiting enzyme for regulation  
455 of the transport of circulating cholesterol and fatty acids, their metabolism and the  
456 turnover of lipoproteins. Perturbations of the placental lipid metabolism have been  
457 connected to pregnancy complications like preeclampsia (Hu et al. 2021). The low  
458 overlap between seahorse and the other two taxa could be due to the different sexes  
459 contributing to the placenta.

460 Changes in expression levels, e.g. of proteins involved in trafficking molecular cargo  
461 between compartments, would be another common adaptation connected to placentation.  
462 Indeed, about 20% of the genes preferentially expressed in human placenta are also found  
463 in the placental transcriptomes of splitfin. Nevertheless, all transcriptomes were enriched  
464 for similar pathways and gene categories, in particular those related to transport across

465 membranes, extracellular matrix, cell interactions and metabolism, but our data do not  
466 point to specific “placentation genes”, which are specifically recruited repeatedly. We  
467 hypothesize that the results may instead indicate that the independent development of  
468 parental provisioning repeatedly made use of genes which already had the same function  
469 in other tissues (e.g. in the transport of metabolites or interaction of between cells and  
470 organs) when it became necessary to make up a novel organ for embryo nutrition. In this  
471 way already pre-existing modules could have been assembled to provide the molecular  
472 changes for the novel trait. This is consistent with the idea that regulatory evolution is  
473 crucial to major evolutionary innovation (Emerson and Li ; Carroll 2008). We have  
474 generated genomic tools for *G. multiradiatus* as a representative of the livebearing  
475 placental goodeids and could identify molecular changes that are connected to this form  
476 of maternal care. Further analysis will benefit from the inclusion of genomes and  
477 transcriptomes of lecithotropic splitfin species and the basal oviparous Goodeidae; the  
478 Empetrichthynae, from which the viviparous splitfins (Goodeinae) diverged 16.8 MYA  
479 (Webb et al 2004).

## 480 **Methods**

### 481 **Experimental Animals**

482 Most samples were from laboratory-born descendants of fish collected in 2011 at Salazar  
483 Lagoon (19°18'26" N, 99°23'20" W, 3000 masl) under license  
484 DGOPA/05332/071007.2437 from Dirección General de Gestión de Pesca y Acuicultura.  
485 We also used, for genome annotation, one sample from an aquarium stock originating  
486 from Zempoala (19°03'00" N, 99°18'42" W) and collected under permit DGOPA  
487 A/01584/110310.0785.

488 Live fish and preserved tissues were exported under permit B00.02.04.-1277.2019 from  
489 the Animal Health Direction (DGSA; SENASICA) of the National Ministry of  
490 Agriculture and Rural Development (SAGARPA).

491 Adult fish were sedated by placing them in ice-cold water, then quickly sacrificed by  
492 decapitation and immediately dissected. Embryos were classified as “early” ( $\leq 4$  weeks of  
493 development) or “late” (five to six weeks of development; gestation lasts around 8 weeks

494 in this species). Embryos were separated from the single ovarian lumen. The  
495 corresponding remaining ovary tissue and trophotaeniae were collected and processed  
496 separately, hence we used whole ovaries from pregnant females, which were free of any  
497 embryonic tissue. For RNA-seq tissues were promptly placed in RNA-later<sup>TM</sup> (2019). For  
498 genome sequencing, dissected organs were flash frozen and stored at -80°C and for RAD-  
499 tag sequencing tissues were stored in 100% ethanol.

500 For whole genome sequencing and assembly three individuals from the same family were  
501 used (Supplemental Table S2).

502 As transcript evidence for genome annotation RNA-seq reads from a total RNA organ  
503 mix of one female (brain, eyes, gills, muscle, skin, kidney, liver, embryos) and ovary  
504 from a second female originating from Zempoala were used.

505 For expression analysis pools of organs and embryos were used (Supplemental Table  
506 S20).

#### 507 **DNA extractions and genome sequencing**

508 Ultralong genomic DNA of different organs of two splitfin individuals was extracted with  
509 the agarose plug based Bionano Prep<sup>TM</sup> Animal tissue kit following the manufacturer's  
510 instructions. Residual pigments were precipitated by adding Triton X-114, SDS and NaCl  
511 to the genomic DNA (Ma et al. 2012). The fragment size of all genomic DNAs was  
512 controlled by pulse-field gel electrophoresis before library construction. Two size-  
513 selected PacBio continuous long read libraries of 24 and 29 kb in size were run on the  
514 SEQUEL system with 10-hour movie times. Linked Illumina reads were generated with  
515 the 10x Genomics Chromium<sup>TM</sup> genome protocol following the manufacturer's  
516 instructions. These libraries were sequenced on the Illumina NovaSeq with a 150bp  
517 paired-end regime. For Bionano optical mapping, genomic DNA was labeled following  
518 the Bionano DLS protocol. Labeled genomic DNAs were run on the Bionano Saphyr  
519 instrument to 200x genome coverage. Hi-C conformation capture of a third individual  
520 was performed following Arima Genomics Hi-C protocol (Arima Hi-C user guide for  
521 Animal tissues, v01), an Illumina library of the enriched regions was prepared with the

522 KAPA HyperPrep Kit, and sequencing was done on an Illumina NovaSeq applying 150  
523 bp paired-end conditions.

524 Details of all protocols are provided in Supplemental Methods: DNA extractions and  
525 genome sequencing.

## 526 **Genome assembly**

527 We assembled the PacBio long reads into contigs using a customized assembler we  
528 termed Damar, a hybrid of the earlier Marvel (Nowoshilow et al. 2018), Dazzler and  
529 Daccord (Tischler and Myers 2017) systems. Next, we used 10x Illumina read-cloud data  
530 to correct base errors and phase haplotypes, arbitrarily picking one haplotype in a phased  
531 block. Afterwards we used Bionano optical maps and then Hi-C data to produce long-  
532 range scaffolds. A manual curation step was performed that uses the Hi-C reads. By  
533 inspecting the Hi-C interaction contact matrix with HiGlass (Kerpedjiev et al. 2018)  
534 remaining false joins were split and curated scaffolds were joined into chromosomes.  
535 Finally, the curated chromosomes were phased by applying an adapted version of the  
536 DipAsm pipeline (Garg et al. 2021).

537 Details of the procedures are provided in Supplemental Methods: Genome assembly.

## 538 **Genome annotation**

539 The genome was annotated using a pipeline adapted from our previous study (Du et al.  
540 2019; Du et al. 2020; Powell et al. 2020). The repeats of the genome were identified and  
541 masked using RepeatModeler, RepeatProteinMask and RepeatMasker  
542 (<http://www.repeatmasker.org>). Then the protein coding genes were annotated by  
543 collecting and synthesizing gene evidence from homology, transcriptome and ab-initio  
544 predictions. Annotated genes were blasted to database InterProscan, Swiss-Prot and  
545 RefSeq for identifying the protein domain and assigning gene symbol and name. At last,  
546 Non-coding RNAs (ncRNAs) were annotated using the method adapted from Ensembl  
547 (<http://ensemblgenomes.org/info/data/ncrna>).

548 Details of the procedures are provided in Supplemental Methods: Genome annotation.

## 549 **Orthology assignment**

550 Orthology of genes were assigned by a clustering of sequence similarity followed by  
551 gene-tree construction in each gene cluster. Sequence similarity was indexed by BLAST  
552 (Camacho et al. 2009) score between protein sequences of each two genes. Clustering  
553 was implemented by `hc_cluster` (Ruan et al. 2007) (Supplemental Fig. S15). Then the  
554 gene tree of each cluster was constructed using TreeBeST (Ponting 2007).

555 Orthology between chromosomes from two species was depicted using Circos diagram  
556 (Krzywinski et al. 2009) based on orthologous genes with conserved synteny.

557 Details of the procedures are provided in Supplemental Methods: Orthology assignment.

### 558 **Phylogenetic analysis**

559 Phylogenetic tree was reconstructed first using maximum-likelihood method  
560 implemented in RAxML (Stamatakis 2014), then confirmed the topology using bayesian  
561 inference implemented in MrBayes (Ronquist et al. 2012). The input data were protein  
562 sequences of 1425 one-to-one orthologs with conserved synteny. We also inferred the  
563 divergence time of species using MCMCTree under a relaxed-clock model (Yang 2007;  
564 Inoue et al. 2011). Two time-calibrations were set: *O. latipes*–*T. nigroviridis* (~96.9–  
565 150.9Ma) and Clupeiformes–Cypriniformes (~185–225Ma) (Near et al. 2012; Lin et al.  
566 2016; Hughes et al. 2018).

567 Details of the procedures are provided in Supplemental Methods: Phylogenetic analysis.

### 568 **Dynamics of gene family size**

569 Gene groups clustered by `Hcluster_sg` were taken as gene families. Together with the  
570 phylogenetic tree built by RAxML and MCMCTree, they were transferred to CAFE5 for  
571 gene family size analysis (Zenodo [https://doi:10.5281/zenodo.3625141](https://doi.org/10.5281/zenodo.3625141), as developed on  
572 GitHub). To estimate the birth-death parameter  $\lambda$ , we only selected gene families that  
573 were present in more than seven species and in each species had less than 100 gene  
574 family members. Then with the previously estimated  $\lambda$ , gene family contraction and  
575 expansion dynamics were accessed for the remaining families. Before  $\lambda$  estimation, an  
576 error model was estimated to account for genome assembly and annotation error.  $\lambda$  was  
577 estimated using Gamma modelling with two categories.

## 578 **RAD-tag sequencing and analysis of sex-specific markers**

579 RAD-tag libraries were built from genomic DNA of 29 females and 27 males, and  
580 sequenced on the HiSeq 2500 platform. The reads were demultiplexed and then  
581 determined present or not in each female and male individual in RADSex (Computing  
582 2013; Feron et al. 2021). A tile plot describing the number of reads in the number of  
583 female/male individuals was then generated and used to reveal the sex-determination  
584 system of the species. Reads that present only in male were then aligned to the genome to  
585 located the sex-determination region.

586 Details of the procedures are provided in Supplemental Methods: RAD-tag sequencing  
587 and analysis of sex-specific markers.

## 588 **RNA extractions and transcriptome sequencing**

589 Total RNA was isolated using TRIzol Reagent (Thermo Fisher Scientific, Waltham,  
590 USA) according to the supplier's recommendation. Custom sequencing (BGI, Shenzhen,  
591 China) of TruSeq libraries generated 30-35 million 150bp paired end clean reads for each  
592 sample on the BGISEQ platform.

## 593 **Differential gene expression analysis**

594 Clean reads were aligned to genome assembly using STAR (`-runMode alignReads -`  
595 `quantMode GeneCounts`) (Dobin et al. 2013) and counted and normalized for each gene  
596 using DESeq2 (Love et al. 2014). Gene with normalized reads count >10 in a tissue was  
597 defined as “expressbased divergence time estimate of splitfined”. Expression with  
598 upregulation of  $\log_2$  fold change >2 in one tissue than in the other was termed as  
599 “enhanced expression” in the former tissue. We pooled the data of early and late stage  
600 embryos and trophotaeniae considering they are tightly grouped together in both  
601 hierarchical clustering and correspondence analysis (Supplemental Fig. S16). For cross-  
602 comparison of detected genes, dataset of human, *Poeciliopsis* and seahorse were retrieved  
603 from previous studies (for details how the datasets were produced see Supplemental table  
604 S21).

605 Details of the procedures are provided in Supplemental Methods: Differential gene  
606 expression analysis.

### 607 **Positive selection**

608 Protein and CDS sequences of genes were downloaded from NCBI (Supplemental Table  
609 S22). Sequences were aligned using MUSCLE (Edgar 2004) and the format was  
610 transformed using an in-house script (Supplemental Code). Positive selection on a gene  
611 of the species was detected using ‘Environment for Tree Exploration’ (ETE3) toolkit  
612 (Huerta-Cepas et al. 2016), which automates CodeML and Slr analyses by using pre-  
613 configured evolutionary models, the species tree and alignment of the orthologous coding  
614 sequences. A gene was identified as a positively-selected gene when it contains sites  
615 (probability > 0.95) of either class 2a (positive selection in marked branch and conserved  
616 in rest) or class 2b (positive selection in marked branch and relaxed in rest).

617 Details of the procedures are provided in Supplemental Methods: Positive selection.

### 618 **Data access**

619 All raw and processed sequencing data generated in this study have been submitted to the  
620 NCBI BioProject database (<https://www.ncbi.nlm.nih.gov/bioproject/>) under  
621 accession number PRJNA768329 and PRJNA745519. The genome assembly generated  
622 in this study has been submitted to the NCBI Assembly database  
623 (<https://www.ncbi.nlm.nih.gov/assembly>) under accession number PRJNA768329. The  
624 genome annotation has been submitted to figshare  
625 ([https://figshare.com/articles/dataset/Girardinichthys\\_multiradiatus\\_201028\\_tar\\_gz/1517](https://figshare.com/articles/dataset/Girardinichthys_multiradiatus_201028_tar_gz/15173181)  
626 3181).

### 627 **Competing interest statement**

628 The authors declare that they have no competing interests.

### 629 **Acknowledgements**

630 We gratefully acknowledge the contribution of the Long Read Team of the DRESDEN-  
631 concept Genome Center, DFG NGS Competence Center, part of the Center for Molecular

632 and Cellular Bioengineering (CMCB), Technische Universität Dresden and MPI-CBG.  
 633 MS was supported by the Deutsche Forschungsgemeinschaft (SCHA 408/10-1). CMG  
 634 received funding from PAPIIT (PAPIIT IN210718), the science funding agency of the  
 635 Universidad Nacional Autónoma de México. MP was funded by the Federal Ministry of  
 636 Education and Research (grant 01IS18026C).

### 637 **Authors' contributions**

638 M. S, C. M. G. and G. M. conceived and designed the project. E. A. L. and C. M. G.  
 639 provided the materials. B. W. and S. W. extracted DNA and RNA samples. S. W.  
 640 conducted the sequencing, M. P. did the assembly and K. D. the annotation. K. D, S. K,  
 641 I.dC. and M. S. analyzed the sequencing data. Y. G. and R. F. did the RADSex analyses.  
 642 K. D, R. F, S. K. S. W. and M. P. prepared figures and tables. C. M. G, M. S. and K. D.  
 643 wrote the manuscript draft, and Y. G. revised it. All authors read and approved the final  
 644 manuscript.

### 645 **References**

- 646 Anchin M, Murcia L, Alcaraz-Pérez F, García-Navarro EM, Cayuela ML. 2011.  
 647 Behaviour of telomere and telomerase during aging and regeneration in  
 648 zebrafish. *PLoS one* **6**: e16955.
- 649 Arellano-Aguilar O, Macías García C. 2008. Correction for Arellano-Aguilar and  
 650 Macías García, Exposure to pesticides impairs the expression of fish  
 651 ornaments reducing the availability of attractive males. *Proceedings of the*  
 652 *Royal Society B: Biological Sciences* **275**: 2899-2899.
- 653 Arellano-Aguilar O, Macías García C. 2008. Exposure to pesticides impairs the  
 654 expression of fish ornaments reducing the availability of attractive males.  
 655 *Proceedings of the Royal Society B: Biological Sciences* **275**: 1343-1351.
- 656 BISAZZA A. 1997. Sexual selection constrained by internal fertilization in the  
 657 livebearing fish *Xenotoca eiseni*. *Animal behaviour* **54**: 1347-1355.
- 658 Blackburn DG. 1999. Are viviparity and egg-guarding evolutionarily labile in  
 659 squamates? *Herpetologica*: 556-573.
- 660 Blackburn DG. 2015. Evolution of vertebrate viviparity and specializations for fetal  
 661 nutrition: a quantitative and qualitative analysis. *Journal of Morphology* **276**:  
 662 961-990.
- 663 Camacho C, Coulouris G, Avagyan V, Ma N, Papadopoulos J, Bealer K, Madden TL.  
 664 2009. BLAST+: architecture and applications. *BMC bioinformatics* **10**: 421.
- 665 Carroll SB. 2008. Evo-devo and an expanding evolutionary synthesis: a genetic  
 666 theory of morphological evolution. *Cell* **134**: 25-36.
- 667 Computing R. 2013. R: A language and environment for statistical computing. *Vienna*:  
 668 *R Core Team*.

- 669 Constantz GD. 1984. Sperm competition in poeciliid fishes. *Sperm competition and*  
670 *the evolution of animal mating systems*: 465-485.
- 671 Darwin C. 1896. *The descent of man and selection in relation to sex*. D. Appleton.
- 672 De La Vega-Salazar MY, Avila-Luna E, Macías-García C. 2003. Ecological evaluation of  
673 local extinction: the case of two genera of endemic Mexican fish,  
674 *Zoogoneticus* and *Skiffia*. *Biodiversity & Conservation* **12**: 2043-2056.
- 675 DeChiara TM, Efstratiadis A, Robertson EJ. 1990. A growth-deficiency phenotype in  
676 heterozygous mice carrying an insulin-like growth factor II gene disrupted by  
677 targeting. *Nature* **345**: 78-80.
- 678 DeChiara TM, Robertson EJ, Efstratiadis A. 1991. Parental imprinting of the mouse  
679 insulin-like growth factor II gene. *Cell* **64**: 849-859.
- 680 Dobin A, Davis CA, Schlesinger F, Drenkow J, Zaleski C, Jha S, Batut P, Chaisson M,  
681 Gingeras TR. 2013. STAR: ultrafast universal RNA-seq aligner. *Bioinformatics*  
682 **29**: 15-21.
- 683 Dobolyi A, Oláh S, Keller D, Kumari R, Fazekas EA, Csikós V, Renner É, Cservenák M.  
684 2020. Secretion and function of pituitary prolactin in evolutionary  
685 perspective. *Frontiers in Neuroscience* **14**: 621.
- 686 DOMÍNGUEZ-DOMÍNGUEZ O, MARTÍNEZ-MEYER E, Zambrano L, DE LEÓN GPP.  
687 2006. Using ecological-niche modeling as a conservation tool for freshwater  
688 species: live-bearing fishes in central Mexico. *Conservation Biology* **20**: 1730-  
689 1739.
- 690 Du K, Stöck M, Kneitz S, Klopp C, Woltering JM, Adolphi MC, Feron R, Prokopov D,  
691 Makunin A, Kichigin I. 2020. The sterlet sturgeon genome sequence and the  
692 mechanisms of segmental rediploidization. *Nature Ecology & Evolution* **4**:  
693 841-852.
- 694 Du K, Wuertz S, Adolphi M, Kneitz S, Stöck M, Oliveira M, Nóbrega R, Ormanns J, Kloas  
695 W, Feron R. 2019. The genome of the arapaima (*Arapaima gigas*) provides  
696 insights into gigantism, fast growth and chromosomal sex determination  
697 system. *Scientific Reports* **9**: 5293.
- 698 Edgar RC. 2004. MUSCLE: multiple sequence alignment with high accuracy and high  
699 throughput. *Nucleic acids research* **32**: 1792-1797.
- 700 Emerson J, Li W-H. The genetic basis of evolutionary change in gene expression.
- 701 Feron R, Pan Q, Wen M, Imarazene B, Jouanno E, Anderson J, Herpin A, Journot L,  
702 Parrinello H, Klopp C. 2021. RADSex: A computational workflow to study sex  
703 determination using restriction site-associated DNA sequencing data.  
704 *Molecular Ecology Resources* **21**: 1715-1731.
- 705 Fragkiadaki P, Tsoukalas D, Fragkiadoulaki I, Psycharakis C, Nikitovic D, Spandidos  
706 DA, Tsatsakis AM. 2016. Telomerase activity in pregnancy complications  
707 (Review). *Mol Med Rep* **14**: 16-21.
- 708 Furness AI, Capellini I. 2019. The evolution of parental care diversity in amphibians.  
709 *Nature communications* **10**: 1-12.
- 710 Garcia CM, Saborío E, Berea C. 1998. Does male-biased predation lead to male  
711 scarcity in viviparous fish? *Journal of Fish Biology* **53**: 104-117.

- 712 Garcia CM, Valero A. 2010. Sexual conflict and sexual selection in the Goodeinae, a  
713 clade of viviparous fish with effective female mate choice. *Advances in the*  
714 *study of behavior* **42**: 1-54.
- 715 Garg S, Fungtammasan A, Carroll A, Chou M, Schmitt A, Zhou X, Mac S, Peluso P,  
716 Hatas E, Ghurye J. 2021. Chromosome-scale, haplotype-resolved assembly of  
717 human genomes. *Nature biotechnology* **39**: 309-312.
- 718 Ghalambor CK, Reznick DN, Walker JA. 2004. Constraints on adaptive evolution: the  
719 functional trade-off between reproduction and fast-start swimming  
720 performance in the Trinidadian guppy (*Poecilia reticulata*). *The American*  
721 *Naturalist* **164**: 38-50.
- 722 González Zuarth C, Macías Garcia C. 2006. Phenotypic differentiation and pre-mating  
723 isolation between allopatric populations of *Girardinichthys multiradiatus*.  
724 *Proceedings of the Royal Society B: Biological Sciences* **273**: 301-307.
- 725 Greven H, Brenner M. 2010. How to copulate without an intromittent organ: the  
726 external genital structures and mating behaviour of *Xenotoca eiseni*  
727 (*Goodeidae*). *Viviparous Fishes II New Life Publications, Homestead, Florida*:  
728 446-450.
- 729 Greven H, Grossherr M. 1992. Adelphophagy and oophagy in *Amea splendens*  
730 Miller & Fitzsimons, 1971 (*Goodeidae*. *Teleostei*). *Z Frischk* **1**: 193-197.
- 731 Griffith O, Wagner G. 2017. The placenta as a model for understanding the origin  
732 and evolution of vertebrate organs. *Nature Ecology & Evolution* **1**: 0072.
- 733 Guernsey MW, van Kruistum H, Reznick DN, Pollux BJ, Baker JC. 2020. Molecular  
734 signatures of placentation and secretion uncovered in *Poeciliopsis* maternal  
735 follicles. *Molecular biology and evolution* **37**: 2679-2690.
- 736 Guerrero-Estévez S, López-López E. 2016. Effects of endocrine disruptors on  
737 reproduction in viviparous teleosts with intraluminal gestation. *Reviews in*  
738 *Fish Biology and Fisheries* **26**: 563-587.
- 739 Guo J, Zhu P, Wu C, Yu L, Zhao S, Gu X. 2003. In silico analysis indicates a similar gene  
740 expression pattern between human brain and testis. *Cytogenet Genome Res*  
741 **103**: 58-62.
- 742 Guo JH, Huang Q, Studholme DJ, Wu CQ, Zhao Z. 2005. Transcriptomic analyses  
743 support the similarity of gene expression between brain and testis in human  
744 as well as mouse. *Cytogenet Genome Res* **111**: 107-109.
- 745 Herpin A, Scharl M. 2008. Regulatory putsches create new ways of determining  
746 sexual development. *EMBO reports* **9**: 966-968.
- 747 Hu M, Li J, Baker PN, Tong C. 2021. Revisiting preeclampsia: a metabolic disorder of  
748 the placenta. *The FEBS Journal*.
- 749 Huerta-Cepas J, Serra F, Bork P. 2016. ETE 3: reconstruction, analysis, and  
750 visualization of phylogenomic data. *Molecular biology and evolution* **33**:  
751 1635-1638.
- 752 Hughes LC, Ortí G, Huang Y, Sun Y, Baldwin CC, Thompson AW, Arcila D, Betancur-R  
753 R, Li C, Becker L. 2018. Comprehensive phylogeny of ray-finned fishes  
754 (*Actinopterygii*) based on transcriptomic and genomic data. *Proceedings of*  
755 *the National Academy of Sciences* **115**: 6249-6254.

- 756 Iida A, Nishimaki T, Sehara-Fujisawa A. 2015. Prenatal regression of the  
757 trophotaenial placenta in a viviparous fish, *Xenotoca eiseni*. *Scientific reports*  
758 **5**: 1-5.
- 759 Inoue J, Dos Reis M, Yang Z. 2011. A step-by-step tutorial: Divergence time  
760 estimation with approximate likelihood calculation using MCMCTREE in  
761 PAML. Citeseer.
- 762 Kerpedjiev P, Abdennur N, Lekschas F, McCallum C, Dinkla K, Strobelt H, Luber JM,  
763 Ouellette SB, Azhir A, Kumar N. 2018. HiGlass: web-based visual exploration  
764 and analysis of genome interaction maps. *Genome biology* **19**: 1-12.
- 765 Kin K, Maziarz J, Chavan AR, Kamat M, Vasudevan S, Birt A, Emera D, Lynch VJ, Ott  
766 TL, Pavlicev M et al. 2016. The Transcriptomic Evolution of Mammalian  
767 Pregnancy: Gene Expression Innovations in Endometrial Stromal Fibroblasts.  
768 *Genome Biology and Evolution* **8**: 2459-2473.
- 769 Krzywinski M, Schein J, Birol I, Connors J, Gascoyne R, Horsman D, Jones SJ, Marra  
770 MA. 2009. Circos: an information aesthetic for comparative genomics.  
771 *Genome research* **19**: 1639-1645.
- 772 Lawton BR, Sevigny L, Oberfell C, Reznick D, O'Neill RJ, O'Neill MJ. 2005. Allelic  
773 expression of IGF2 in live-bearing, matrotrophic fishes. *Development genes*  
774 *and evolution* **215**: 207-212.
- 775 Li H, Liang Z, Yang J, Wang D, Wang H, Zhu M, Geng B, Xu EY. 2019. DAZL is a master  
776 translational regulator of murine spermatogenesis. *Natl Sci Rev* **6**: 455-468.
- 777 Lin Q, Fan S, Zhang Y, Xu M, Zhang H, Yang Y, Lee AP, Woltering JM, Ravi V, Gunter  
778 HM. 2016. The seahorse genome and the evolution of its specialized  
779 morphology. *Nature* **540**: 395.
- 780 Lombardi J, Wourms JP. 1985. The trophotaenial placenta of a viviparous goodeid  
781 fish. II. Ultrastructure of trophotaeniae, the embryonic component. *Journal of*  
782 *morphology* **184**: 293-309.
- 783 Love MI, Huber W, Anders S. 2014. Moderated estimation of fold change and  
784 dispersion for RNA-seq data with DESeq2. *Genome biology* **15**: 550.
- 785 Lynch VJ, Tanzer A, Wang Y, Leung FC, Gellersen B, Emera D, Wagner GP. 2008.  
786 Adaptive changes in the transcription factor HoxA-11 are essential for the  
787 evolution of pregnancy in mammals. *Proceedings of the National Academy of*  
788 *Sciences* **105**: 14928-14933.
- 789 Ma R, Zhao J, Du H-C, Tian S, Li L-W. 2012. Removing endotoxin from plasmid  
790 samples by Triton X-114 isothermal extraction. *Analytical biochemistry* **424**:  
791 124-126.
- 792 Macías-García C, Saborío E. 2004. Sperm competition in a viviparous fish.  
793 *Environmental Biology of Fishes* **70**: 211-217.
- 794 Marina Y, Tabche LMn, García CMA. 1997. Bioaccumulation of methyl parathion and  
795 its toxicology in several species of the freshwater community in Ignacio  
796 Ramirez dam in Mexico. *Ecotoxicology and environmental safety* **38**: 53-62.
- 797 Matos B, Publicover SJ, Castro LFC, Esteves PJ, Fardilha M. 2021. Brain and testis:  
798 more alike than previously thought? *Open Biology* **11**: 200322.
- 799 Mayr E. 1942. Systematics and the Origin of Species. *Columbia University Press, New*  
800 *York*.

- 801 Méndez-Janovitz M, Garcia CM. 2017. Do male fish prefer them big and colourful?  
802 Non-random male courtship effort in a viviparous fish with negligible  
803 paternal investment. *Behavioral Ecology and Sociobiology* **71**: 1-12.
- 804 Méndez-Janovitz M, Gonzalez-Voyer A, Macías Garcia C. 2019. Sexually selected  
805 sexual selection: Can evolutionary retribution explain female ornamental  
806 colour? *Journal of evolutionary biology* **32**: 833-843.
- 807 Mendoza G. 1972. The fine structure of an absorptive epithelium in a viviparous  
808 teleost. *Journal of morphology* **136**: 109-129.
- 809 Meyer A, Lydeard C. 1993. The evolution of copulatory organs, internal fertilization,  
810 placenta and viviparity in killifishes (Cyprinodontiformes) inferred from a  
811 DNA phylogeny of the tyrosine kinase gene X-src. *Proceedings of the Royal  
812 Society of London Series B: Biological Sciences* **254**: 153-162.
- 813 Mossman H. 1991. Comparative morphogenesis of the fetal membranes and  
814 accessory uterine structures. *Placenta* **12**: 1-5.
- 815 Near TJ, Eytan RI, Dornburg A, Kuhn KL, Moore JA, Davis MP, Wainwright PC,  
816 Friedman M, Smith WL. 2012. Resolution of ray-finned fish phylogeny and  
817 timing of diversification. *Proceedings of the National Academy of Sciences* **109**:  
818 13698-13703.
- 819 Nowoshilow S, Schloissnig S, Fei J-F, Dahl A, Pang AW, Pippel M, Winkler S, Hastie  
820 AR, Young G, Roscito JG. 2018. The axolotl genome and the evolution of key  
821 tissue formation regulators. *Nature* **554**: 50-55.
- 822 Panhuis TM, Butlin R, Zuk M, Tregenza T. 2001. Sexual selection and speciation.  
823 *Trends in ecology & evolution* **16**: 364-371.
- 824 Parenti LR. 1981. A phylogenetic and biogeographic analysis of cyprinodontiform  
825 fishes (Teleostei, Atherinomorpha). *Bulletin of the American Museum of  
826 Natural History*.
- 827 Pollux B, Meredith R, Springer M, Garland T, Reznick D. 2014. The evolution of the  
828 placenta drives a shift in sexual selection in livebearing fish. *Nature* **513**:  
829 233-236.
- 830 Pollux B, Pires M, Banet A, Reznick D. 2009. Evolution of placentas in the fish family  
831 Poeciliidae: an empirical study of macroevolution. *Annu Rev Ecol Evol Syst* **40**:  
832 271-289.
- 833 Ponting C. 2007. TreeBeST: Tree building guided by Species Tree.
- 834 Powell DL, García-Olazábal M, Keegan M, Reilly P, Du K, Díaz-Loyo AP, Banerjee S,  
835 Blakkan D, Reich D, Andolfatto P. 2020. Natural hybridization reveals  
836 incompatible alleles that cause melanoma in swordtail fish. *Science* **368**: 731-  
837 736.
- 838 Rhie A, McCarthy SA, Fedrigo O, Damas J, Formenti G, Koren S, Uliano-Silva M, Chow  
839 W, Fungtammasan A, Kim J. 2021. Towards complete and error-free genome  
840 assemblies of all vertebrate species. *Nature* **592**: 737-746.
- 841 Ritchie MG. 2007. Sexual selection and speciation. *Annu Rev Ecol Evol Syst* **38**: 79-  
842 102.
- 843 Ritchie MG, Webb SA, Graves JA, Magurran AE, Macias Garcia C. 2005. Patterns of  
844 speciation in endemic Mexican Goodeid fish: sexual conflict or early radiation?  
845 *Journal of Evolutionary Biology* **18**: 922-929.

- 846 Ronquist F, Teslenko M, Van Der Mark P, Ayres DL, Darling A, Höhna S, Larget B, Liu  
847 L, Suchard MA, Huelsenbeck JP. 2012. MrBayes 3.2: efficient Bayesian  
848 phylogenetic inference and model choice across a large model space.  
849 *Systematic biology* **61**: 539-542.
- 850 Ruan J, Li H, Chen Z, Coghlan A, Coin LJM, Guo Y, Heriche J-K, Hu Y, Kristiansen K, Li  
851 R. 2007. TreeFam: 2008 update. *Nucleic acids research* **36**: D735-D740.
- 852 Rueda-Jasso RA, los Santos-Bailón D, Fuentes-Farias AL, Gutierrez-Ospina G. 2014.  
853 Toxicidad letal y subletal del fosfato de sodio dibásico y efectos en branquias  
854 y conducta de las crías del pez goodeido *Skiffia multipunctata*. *Hidrobiológica*  
855 **24**: 207-214.
- 856 Saldivar Lemus Y, Vielle-Calzada JP, Ritchie MG, Macías Garcia C. 2017. Asymmetric  
857 paternal effect on offspring size linked to parent-of-origin expression of an  
858 insulin-like growth factor. *Ecol Evol* **7**: 4465-4474.
- 859 Schindler J, Kujat R. 1990. Structure and function of the trophotaenial placenta in  
860 the goodeid teleost, *Skiffia bilineata*. *Jahrbuch für Morphologie und*  
861 *mikroskopische Anatomie 2 Abteilung, Zeitschrift für mikroskopisch-*  
862 *anatomische Forschung* **104**: 241-257.
- 863 Schindler JF. 2003. Scavenger receptors facilitate protein transport in the  
864 trophotaenial placenta of the goodeid fish, *Ameca splendens* (Teleostei:  
865 Atheriniformes). *Journal of Experimental Zoology Part A: Comparative*  
866 *Experimental Biology* **299**: 197-212.
- 867 Schindler JF. 2015. Structure and function of placental exchange surfaces in goodeid  
868 fishes (Teleostei: Atheriniformes). *Journal of morphology* **276**: 991-1003.
- 869 Schindler JF, De Vries U. 1987. Protein uptake and transport by trophotaenial  
870 absorptive cells in two species of goodeid embryos. *Journal of Experimental*  
871 *Zoology* **241**: 17-29.
- 872 Shao F, Wang J, Xu H, Peng Z. 2018. FishTEDB: a collective database of transposable  
873 elements identified in the complete genomes of fish. *Database* **2018**.
- 874 Simmons LW, Fitzpatrick JL. 2012. Sperm wars and the evolution of male fertility.  
875 *Reproduction* **144**: 519.
- 876 Sreenivasan R, Cai M, Bartfai R, Wang X, Christoffels A, Orban L. 2008.  
877 Transcriptomic analyses reveal novel genes with sexually dimorphic  
878 expression in the zebrafish gonad and brain. *PLoS One* **3**: e1791.
- 879 Stamatakis A. 2014. RAxML version 8: a tool for phylogenetic analysis and post-  
880 analysis of large phylogenies. *Bioinformatics* **30**: 1312-1313.
- 881 Tischler G, Myers EW. 2017. Non hybrid long read consensus using local de Bruijn  
882 graph assembly. *bioRxiv*: 106252.
- 883 Turner C. 1937. Reproductive cycles and superfetation in poeciliid fishes. *The*  
884 *Biological Bulletin* **72**: 145-164.
- 885 Uribe M, Aguilar-Morales M, De la Rosa-Cruz G, García-Alarcón A, Campuzano-  
886 Caballero J, Guerrero-Estévez S. 2010. Ovarian structure and embryonic  
887 traits associated with viviparity in poeciliids and goodeids. *Viviparous fishes*  
888 *II*: 211-229.
- 889 Uribe MC DIR-CG, García-Alarcón A. 2005. The ovary of viviparous teleost.  
890 Morphological differences between the ovaries of *Goodea atripinnis* and

- 891 Ilyodon whitei (Goodeidae). In *Viviparous Fishes*, (ed. GH Uribe MC), pp. 217-  
892 235. New Life Publications, Homestead, Florida.
- 893 Uyeno T, Miller RR, Fitzsimons JM. 1983. Karyology of the Cyprinodontoid Fishes of  
894 the Mexican Family Goodeidae. *Copeia* **1983**: 497-510.
- 895 van Kruistum H, van den Heuvel J, Travis J, Kraaijeveld K, Zwaan BJ, Groenen MA,  
896 Megens H-J, Pollux BJ. 2019. The genome of the live-bearing fish *Heterandria*  
897 *formosa* implicates a role of conserved vertebrate genes in the evolution of  
898 placental fish. *BMC evolutionary biology* **19**: 1-11.
- 899 Vega-López A, Ortiz-Ordóñez E, Uría-Galicia E, Mendoza-Santana EL, Hernández-  
900 Cornejo R, Atondo-Mexia R, García-Gasca A, García-Latorre E, Domínguez-  
901 López ML. 2007. The role of vitellogenin during gestation of *Girardinichthys*  
902 *viviparus* and *Ameca splendens*; two goodeid fish with matrotrophic  
903 viviparity. *Comparative Biochemistry and Physiology Part A: Molecular &*  
904 *Integrative Physiology* **147**: 731-742.
- 905 Webb SA, Graves JA, Macias-Garcia C, Magurran AE, Foighil DÓ, Ritchie MG. 2004.  
906 Molecular phylogeny of the livebearing Goodeidae (Cyprinodontiformes).  
907 *Molecular phylogenetics and evolution* **30**: 527-544.
- 908 Whittington CM, Griffith OW, Qi W, Thompson MB, Wilson AB. 2015. Seahorse brood  
909 pouch transcriptome reveals common genes associated with vertebrate  
910 pregnancy. *Molecular Biology and Evolution* **32**: 3114-3131.
- 911 Whittington CM, Wilson AB. 2013. The role of prolactin in fish reproduction. *General*  
912 *and comparative endocrinology* **191**: 123-136.
- 913 Wright WE, Piatyszek MA, Rainey WE, Byrd W, Shay JW. 1996. Telomerase activity  
914 in human germline and embryonic tissues and cells. *Developmental genetics*  
915 **18**: 173-179.
- 916 Yang Z. 2007. PAML 4: phylogenetic analysis by maximum likelihood. *Molecular*  
917 *biology and evolution* **24**: 1586-1591.
- 918 Yuan XN, Jiang XY, Pu JW, Li ZR, Zou SM. 2011. Functional conservation and  
919 divergence of duplicated insulin-like growth factor 2 genes in grass carp  
920 (*Ctenopharyngodon idellus*). *Gene* **470**: 46-52.

## 921 **Figure legends**

922 Fig. 1. Images of a pregnant female adult of darkedged splitfin, one laid embryo with the  
923 trophotaeniae and a schematic drawing of the ovary/placental organ. For detail of the  
924 organ structure, see Figures 31-33 in Uribe, Aguilar-Morales et al. 2010. For comparison  
925 of the placental organs in mammals, seahorse and poeciliid fishes, see Figure 3 in  
926 Griffith&Wagner 2017.

927 Fig. 2. Hi-C contact heat map of the scaffolded portion of the splitfin genome assembly.

928 Fig. 3. Species tree and Chord diagrams showing orthology between *Girardinichthys*  
929 *multiradiatus* and other teleost species. For each species, chromosome orthology to *G.*

930 *multiradiatus* is shown in a chord diagram, where blocks on circumference represent  
931 chromosomes, coloured threads link orthologous genes with conserved synteny.  
932 Chromosomes of *G. multiradiatus* are represented by coloured blocks while those of  
933 other species are in black. Bootstrap support values are labeled on each node. Scale bar  
934 indicates average substitutions per site. Branches leading to live-bearing species are  
935 marked with purple four-pointed stars.

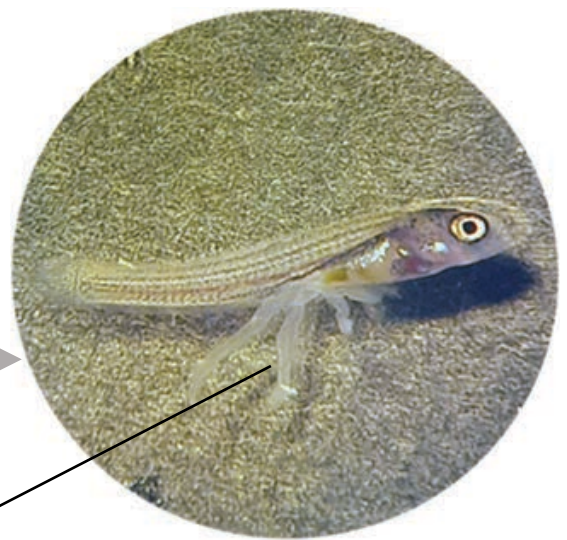
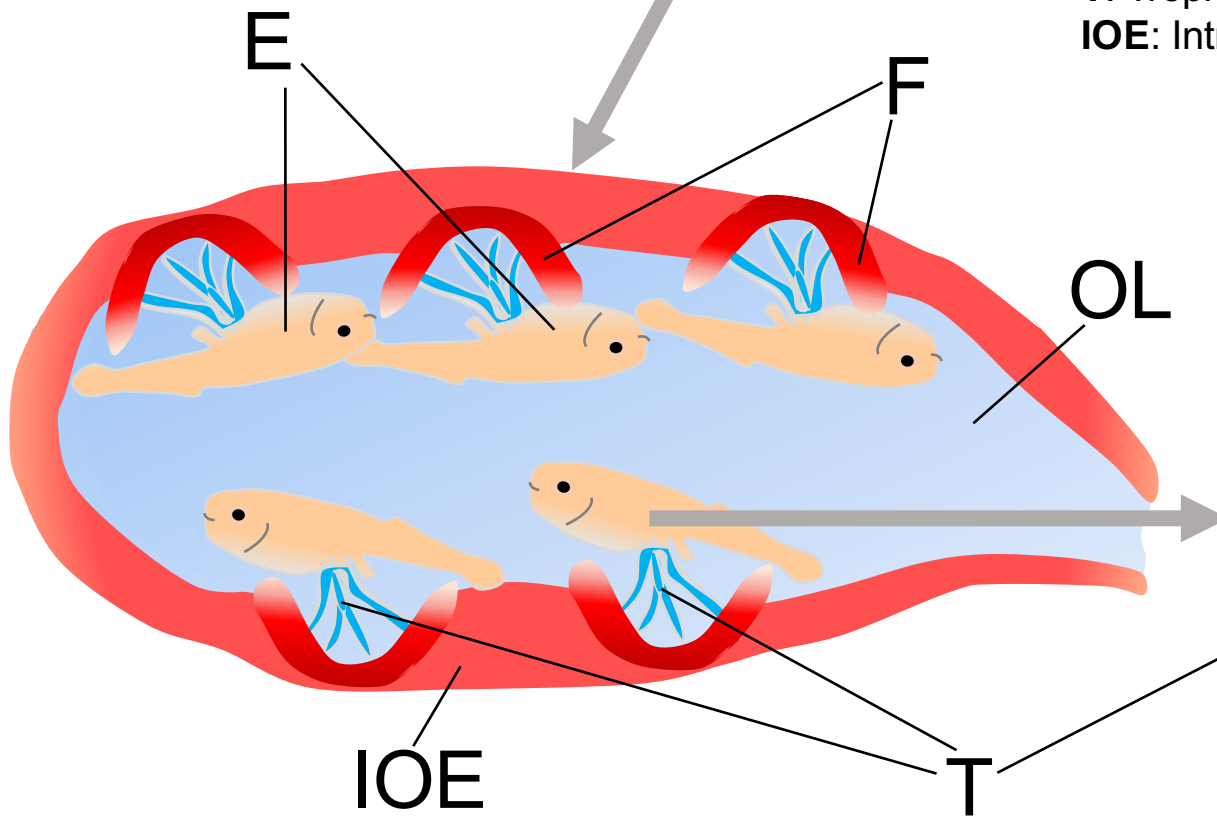
936 Fig. 4. Identification of the sex chromosomes by RAD-tag sequencing. (A) Distribution  
937 of RADSex markers between males (horizontal axis) and females (vertical axis) using a  
938 minimum depth of 1 to consider a marker present in an individual. There were 892  
939 markers significantly associated with male phenotypes in the tiles highlighted in red. (B)  
940 Manhattan plot showing the negative log of p-value of association with sex for all  
941 RADSex markers aligned to the genome. The vast majority of aligned markers  
942 significantly associated with sex (97%) was aligned to scaffold\_20. (C) Negative log of  
943 p-value of association with sex for all RADSex markers aligned to scaffold\_20. Markers  
944 significantly associated with sex aligned to a continuous region spanning from the start of  
945 the chromosome to ~32.5 Mb.

946 Fig. 5. Circos and dot plots showing synteny and sequence difference between  
947 Chromosome X and Y. (A) Circos plot of Chromosomes 18 to 24 and both haplotypes of  
948 scaffold 20 (X and Y) showing repeat content (gray histogram), GC value (black  
949 histogram), male-specific RAD-tag hits (red bars) and synteny (linking ribbon) on  
950 chromosomes; with in middle the image of a male darkedged splitfin adult. (B) Dot plots  
951 showing the sequence difference (percentage of SNPs and indels in windows of size  
952 100k) between X and Y.

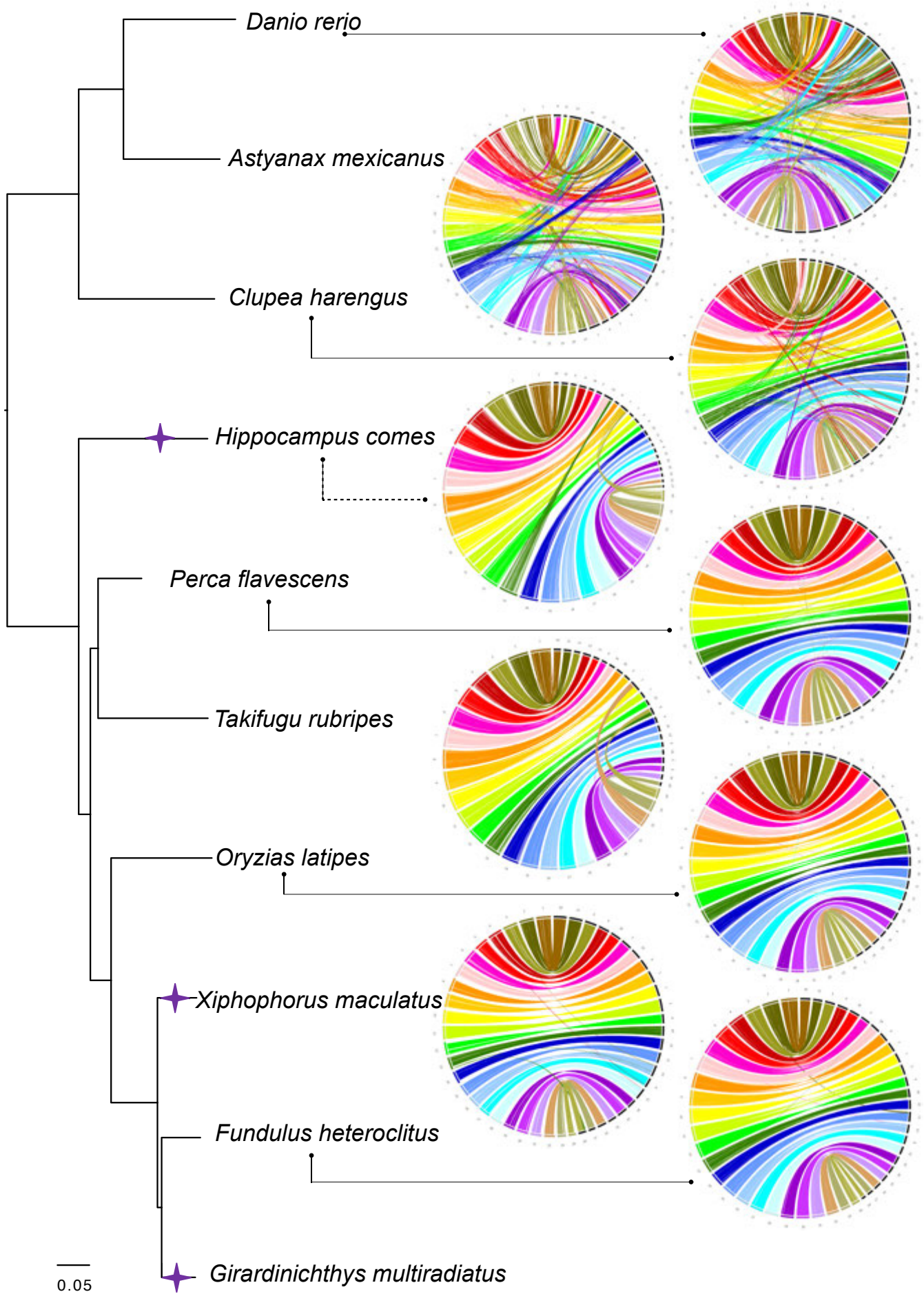
953

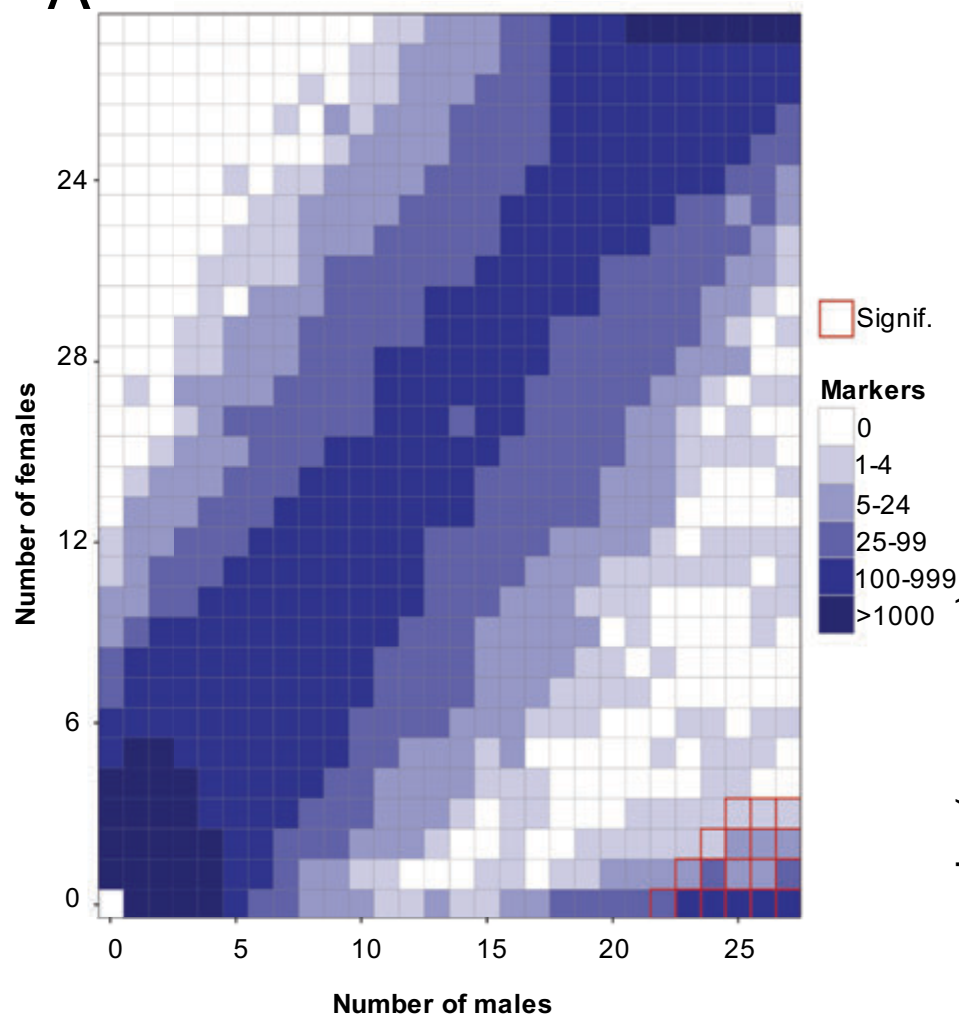
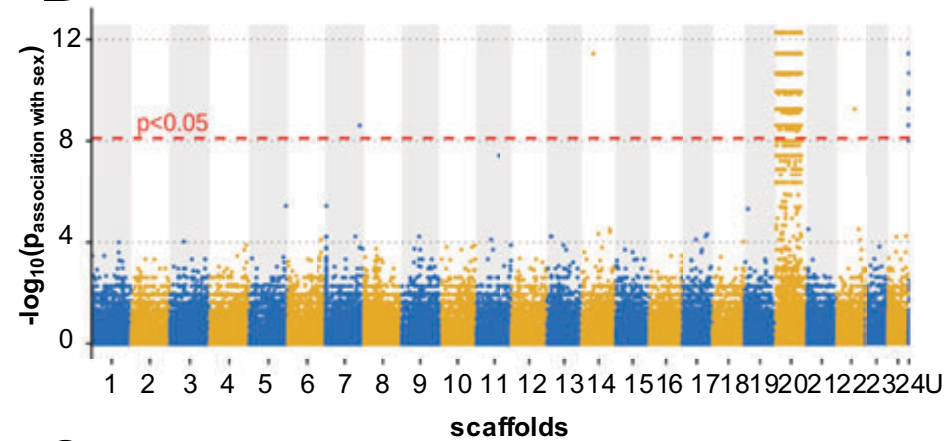


**E:** Embryos  
**F:** Folicle (ruptured -ovulation- shortly after fertilisation)  
**OL:** Ovarian lumen  
**T:** Trophotaeniae  
**IOE:** Intra-ovarian epithelium







**A****B****C**